Permeability testing of biomaterial membranes

L Dreesmann[1], R Hajosch[1], M Ahlers[2], J Vaz Nuernberger[1] and B Schlosshauer[1,3]

[1] NMI Natural and Medical Sciences Institute at the University Tübingen, Markwiesenstr. 55, D-72770 Reutlingen, Germany
[2] GELITA AG, Gammelsbacher Str. 2, D-69412 Eberbach, Germany

E-mail: schlosshauer@nmi.de

Abstract
The permeability characteristics of biomaterials are critical parameters for a variety of
implants. To analyse the permeability of membranes made from crosslinked ultrathin gelatin
membranes and the transmigration of cells across the membranes, we combined three
technical approaches: (1) a two-chamber-based permeability assay, (2) cell culturing with
cytochemical analysis and (3) biochemical enzyme electrophoresis (zymography). Based on
the diffusion of a coloured marker molecule in conjunction with photometric quantification,
permeability data for a gelatin membrane were determined in the presence or absence of
gelatin degrading fibroblasts. Cytochemical evaluation after cryosectioning of the membranes
was used to ascertain whether fibroblasts had infiltrated the membrane inside. Zymography
was used to investigate the potential release of proteases from fibroblasts, which are known to
degrade collagen derivatives such as gelatin. Our data show that the diffusion equilibrium of a
low molecular weight dye across the selected gelatin membrane is approached after about
6–8 h. Fibroblasts increase the permeability due to cavity formation in the membrane inside
without penetrating the membrane for an extended time period (>21 days *in vitro*).
Zymography indicates that cavity formation is most likely due to the secretion of matrix
metalloproteinases. In summary, the combination of the depicted methods promises to
facilitate a more rational development of biomaterials, because it provides a rapid means of
determining permeability characteristics and bridges the gap between descriptive methodology
and the mechanistic understanding of permeability alterations due to biological degradation.

(Some figures in this article are in colour only in the electronic version)

1. Introduction

Biomaterials gain increasing importance in the design of biomedical devices and implants. In those cases where biomaterials represent interfaces between different functionally interacting compartments, such as a cell-containing lumen and the surrounding host tissue, the permeability across the biomaterial interface plays a critical role in determining performance and success. This aspect becomes even more demanding with resorbable implants which allow penetration of low-molecular weight metabolites, but prevent transiently cell infiltration or emigration of encapsulated cells. To accelerate the development of biomaterial-based implants, methods performed prior to animal experimentation are required that provide insight into causal links between the biomaterial structure, physical performance and biological responses.

Diffusion of pharmaceuticals across biomaterials is a key issue where retarded and long-term drug delivery is envisaged from drug-containing capsules with permeability cut-offs often below 1 kDa [1, 2]. More advanced approaches use living producer cells as pharmacological active depots [3, 4], whose focus is on macromolecular components including newly

[3] Corresponding address: NMI Naturwissenschaftliches und Medizinisches Institut, an der Universität Tübingen, Markwiesenstr. 55, D-72770 Reutlingen, Germany.

synthesized proteins, with semipermeability ranges typically from 10 to 100 kDa. To treat anaemia, for example, genetically engineered C2C12 myoblasts which secrete erythropoietin (Epo) have been implanted subcutaneously in mice. The cells were encapsulated within semipermeable polyethersulfone hollow fibres [5]. Systemically applied Epo restored haemopoiesis in the state of anaemia due to severe renal failure. In a similar fashion, encapsulated C2C12 myoblasts have been implanted which expressed increased levels of vascular endothelial growth factor (VEGF) and fibroblasts growth factor (FGF-2). Both factors enhanced vascularization and consequently survival in a model of skin flap ischemia [6].

A critical aspect of any implantation strategy is the potential host versus graft rejection. Thus, not only the diffusion of agents out of the implant but also the permeability for immunological relevant components, such as immunoglobulins and cytokines, into the implant compartment need to be considered. Various cases have been reported where immunosuppression was pivotal for the survival of encapsulated cells and the release of effector agents [7, 8]. This aspect is of minor relevance in immune-privileged tissues such as the central nervous system. Encapsulated bovine chromaffin cells have been implanted into the arachnoid space of rats and sheep without the need of immunosuppression. Since these cells release opioid peptides, such implants have the potential to suppress cancer pain [9–11].

Another concern is the stability of the encapsulating biomaterial and changes in its semipermeability. Semipermeability could be reduced by a progressive fouling due to deposits of cellular components accumulating in nano- or micropores of the biomaterial [12, 13]. Conversely, resorbable biomaterials become progressively degraded, and thus an increase in semipermeability should be expected. Understanding the biochemical process of biomaterial degradation/resorption, including its kinetics, is important to enable modification of the material structure (e.g. the degree and type of crosslinking) on a rational basis and thus to change its resorption with or without changing its semipermeability as required [14–16].

We are specifically interested in the development of nerve guides in order to bridge lesion gaps originating from iatrogenic, accidental or disease-related impact. Typically, such nerve guides represent tubular implants that are integrated between the ends of severed nerves [17]. As reviewed recently, some of these implants have already been approved for clinical application in humans [18]. Semipermeability of the tube wall is considered to be crucial for cell survival inside the tube by guaranteeing nutrient diffusion and an oxygen content above 2 μg ml^{-1} [19, 20]. Concomitantly, such implants aim to exclude adverse cell infiltration by fibroblasts from the surrounding tissue, which tends to produce growth inhibitory extracellular matrix components as typically observed in scar tissue [21, 22]. Consequently, during the development of nerve guides it has become very helpful to evaluate at an early stage transmural permeability characteristics and possibly identify mechanisms of biomaterial degradation. In the current report, a combination of three methods is described to address these issues.

2. Material and methods

2.1. Materials

Foetal calf serum, Hanks balanced salt solution (HBSS), phosphate buffered saline without calcium/magnesium (PBS^{-}), 100× penicillin/streptomycin and L-glutamine were purchased from PAA, Linz, Austria. Paraformaldehyde (PFA) was from Merck, Darmstadt, Germany. DNA/nucleus stain 4,6-diaminido-2-phenylindol (DAPI) was from Sigma, Deisenhofen, Germany. Dulbecco's modified Eagle medium (DMEM) was from BioWhittaker™, Verviers, Belgium. Mounting medium PermaFlour was purchased from Dianova/Jackson ImmunoResearch, Hamburg, Germany.

2.2. Gelatin processing

Type A gelatin soft membranes were prepared from porcine skin gelatin (Bloom 300 g, viscosity 4.5 mPa s in a 6.6% solution at 60 °C). Crosslinking was performed by the addition of methanal to gelatin solutions (3000–8000 ppm). To produce gelatin membranes, gelatin solutions of 24% concentration were casted at 60 °C applying a film coater (Erichsen Coatmaster 509/MC-III) which was tempered at 25 °C. The height of the solution casted onto the coater was 200 μm. Gelation of the solution was performed at 25 °C for 1 h. The resulting membranes were dried for 24 h in a conditioning cabinet at 30 °C and 30% relative humidity. Gelatin membranes were transferred to a downstream hardening cabinet with a methanal gas phase (2–17 h, 22 °C). Storage under stress conditions (50 °C, 80% r.h. and 50 °C in vacuum) completed the hardening process. The final thickness of gelatin membranes was about 50 μm. After production, gelatin specimens were pre-conditioned with a culture medium containing 10% serum (3 × 30 min, 37 °C) which induced some swelling and increased the flexibility of membranes.

2.3. Cell culturing

Fibroblasts were isolated from skin of neonatal Lewis rats. Dissected tissue fragments were put onto non-coated Petri dishes with a minimum of fluid for 20 min at 37 °C. Afterwards, a culture medium (DMEM, 10% FCS, 2 mM L-glutamine, 100 U ml^{-1} penicillin/100 μg ml^{-1} streptomycin or 50 μg ml^{-1} gentamycin) was added. After cultivation (37 °C, 5% CO$_2$) for 7 days, tissue explants were removed and fibroblasts that had emigrated from the explants were harvested for expansion. Cells were collected by centrifugation and stored under liquid nitrogen. For some experiments, human foreskin fibroblasts (kindly provided by S Glock, NMI) were employed. Fibroblasts were seeded onto pre-conditioned gelatin membranes and cultured in the above culture medium for 1–21 days before testing the cell-seeded membranes in diffusion assays, cryosectioning or cell staining of whole mounts.
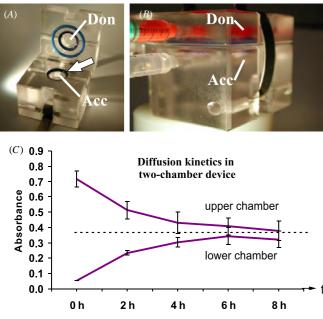
Figure 1. Diffusion chamber. (*A*) Polycarbonate diffusion chamber with a donor chamber (Don) which ultimately harbours buffer with a coloured marker agent and an acceptor chamber (Acc) in the lower block. The biomaterial membrane fixed in o-rings (not shown) is positioned on top of the acceptor chamber (arrow). After closure of the lid, a metal clamp compresses both half-chambers and thus guarantees complete sealing. (*B*) Closed diffusion chamber with a red marker solution (food colouring for demonstration) in the donor chamber. (*C*) The diffusion graph displays the decrease of the marker concentration in the donor chamber over a time period of 8 h (upper graph) and concomitantly the increase in the marker concentration in the acceptor chamber (lower graph). The interface in this control experiment was a nylon mesh with 20 μm spacing. For quantitative analysis, the permeability coefficient (the time-dependent change of marker concentration) was calculated. Mean values $\pm$ standard deviation, $n = 3$.

2.4. Permeability assay

To test diffusion across gelatin membranes, a two-chamber system (Minucells and Minutissue, Bad Abbach, Germany) was employed as previously described [23, 24]. Briefly, gelatin membranes were fixed between two specific o-rings with an operational area of 7 mm² that fitted exactly into the chamber system. The diameter of the biomaterial membrane was about 7 mm. The o-rings were positioned onto the lower chamber, and the polycarbonate lid containing the upper chamber was closed and fastened with a metal clamp (figure 1). Integrated rubber rings ensured that the chamber was completely sealed, and allowed diffusion from the upper to the lower chamber only via penetration through the gelatin membrane, which thus functioned as an interphase. The upper chamber was filled with phenol red-containing buffer via a lateral opening using a syringe, whereas the lower chamber was filled with buffer without dye. Experiments were performed at 37 °C for different time periods up to 8 h as indicated below. Samples collected from the upper and lower chambers were analysed photometrically at 558 nm (Photometer Uvikon 923, Kontron Instruments, Ludwigshafen, Germany). As interfaces, we used either a nylon mesh (20 μm mesh width; Reichelt Chemietechnik,

Heidelberg, Germany), sole gelatin membranes or gelatin membranes seeded with cells for different time periods (see above). The permeability index was calculated according to the formula

$$P_e = \mathrm{d}x/\mathrm{d}t \times (C \times A)^{-1},$$

where P_e is the permeability coefficient (cm s^{-1}), dx/dt is the rate of translocation (pmol s^{-1}), C is the initial concentration of the dye in the donor chamber (pmol cm^{-3}) and A is the area of penetration (cm²). For additional analysis, some gelatin membranes were further processed by cytochemical means (see below).

2.5. Cytochemistry

To address the structural changes of gelatin membranes seeded with fibroblasts, specimens were fixed in 4% PFA/PBS (24 h, r.t.), impregnated in 30% sucrose and embedded in TissueTek before micro-sectioning (10–20 μm) in a cryostat (Leica) at −18 °C. Collected sections were immobilized on coated glass slides. For the analysis of whole mounts, specimens were fixed identically, washed, permeabilized (0.2% TX-100), blocked (1% BSA/PBS) and incubated with phalloidin (Sigma, Germany) against F-actin and counterstained with DAPI as outlined previously [25]. Quantification of mass loss was based on area measurements (given as kilopixel—kPi) of digitized cryosections of gelatin membranes after culturing with or without fibroblasts (AxioVision$^{\mathrm{TM}}$, Zeiss, Oberkochen, Germany).

2.5.1. Zymography. The proteolytic activity of cell cultures was analysed by zymography according to the manufacturers' instructions (Novex® Zymogram Gels, Invitrogen, Carlsbad, CA, USA). Briefly, pre-casted 10% acrylamide tris-glycine gels with incorporated 0.1% gelatin as a metalloproteinase substrate were employed in a Xcell SureLock Mini-cell System (Invitrogen). Cell culture supernatants were collected from confluent human foreskin fibroblasts cultured on gelatin membranes as outlined above, denatured in SDS buffer under non-reducing conditions and electrophoresed without heating using the tris-glycine SDS running buffer (125 V, 90 min). Positive controls contained purified collagenase B (from clostridium histolyticum, Roche; 11088807001) in buffer. As marker proteins, SeeBlue®Plus2 Prestained Standard (Invitrogen, Carlsbad, CA, USA) were used. After the run was complete, the enzyme activity was renatured by incubating the gel in *zymogram renaturing buffer* (Bio-Rad) containing a non-ionic detergent for 30 min at room temperature with gentle agitation. After equilibration in *zymogram developing buffer* (Bio-Rad) for 30 min, the gel was incubated at 37 °C overnight for maximum sensitivity. In parallel, some gels were incubated with the potent broad spectrum matrix metalloproteinase (MMP) inhibitor GM 6001 Galardin in all buffers (dilution 1:1000; BIOMOL International, USA). Gels were stained with Coomassie brilliant blue R-250 (0.5%) and partially destained thereafter. Since the incorporated gelatin caused ubiquitous blue staining, protease bands where gelatin had been degraded appeared as clear bands against the

medium-blue background. Marker proteins were heavily blue stained. Stained gels were scanned and the digitized image evaluated.

3. Results

3.1. Gelatin membrane permeability

The first set of experiments were performed to determine baseline features of the diffusion device for biomaterial testing. The principal components are two polycarbonate blocks with half-chambers: one in the base and one in the lid (figure 1). The half-chambers represent individual compartments, once a separating interface such as a test membrane has been placed between the chambers (arrow in figure 1(*A*)) and after closure of the device. Both compartments can be hermetically sealed after the lid has been latched with the single metal clamp and can be fed with different solutions via four openings. The upper (donor) chamber was filled with a medium containing phenol red as a diffusion marker, whereas the lower (acceptor) chamber was filled with pure buffer. To determine the time course of largely unaffected diffusion, a nylon mesh with 20 μm spacing was employed which prevented intermixing during sample application on the one hand, but was considered not to hamper diffusion. Samples were collected at five different time points. As depicted in figure 1, after about 6–8 h the system approached an equilibrium state. For this and subsequent experiments, the permeability coefficient was calculated from the relative difference in absorbance (i.e. concentration of phenol red) between the donor and the acceptor chambers. The permeability coefficient (see section 2) for phenol red in this setting was $2.81 \times 10^{-4} \pm 1.39 \times 10^{-4}$.

When nylon meshes were compared with gelatin membranes (thickness 50 μm), reduced permeability became evident ($1.30 \times 10^{-4} \pm 0.26 \times 10^{-4}$ versus $2.81 \times 10^{-4} \pm 1.39 \times 10^{-4}$). Because gelatin membranes will be part of future nerve guide implants, it is important to know whether the presence of cells plays a role in altering the permeability characteristics. Therefore, fibroblasts were seeded onto gelatin membranes and cultured for different time periods in static cultures (up to 3 weeks). Thereafter, cell-seeded membranes were inserted into the diffusion chamber (figure 2(*A*)). It will be seen that the addition of fibroblasts increased the permeability significantly. The permeability coefficient increased nearly threefold during a 3 week incubation period (figure 2(*B*)). The change in permeability is likely to be related to a combined effect of cell-dependent and cell-independent biomaterial alterations, because even without cells the permeability increased after 3 weeks *in vitro*. However, this change was considerably slower, since during a 24 h period cells caused a nearly 30% faster increase in permeability than pure buffer exposure in 3 weeks. For both 3 week exposures, the permeability coefficients for phenol red increased to $2.26 \times 10^{-4} \pm 0.40 \times 10^{-4}$ in the absence of cells and to $3.75 \times 10^{-4} \pm 1.27 \times 10^{-4}$ in the presence of fibroblasts. In summary, under the experimental conditions, fibroblasts did not encapsulate the interface and thus did not decrease the gelatin membrane permeability, but rather increased it.
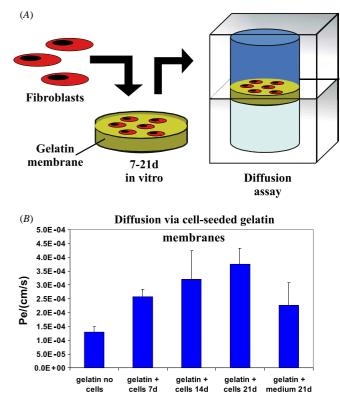

Figure 2. Impact of fibroblasts on the permeability of a gelatin membrane. (*A*) Schematic representation of the experimental layout. Fibroblasts were collected and seeded onto gelatin membranes and cultured for different time periods. Afterwards, fibroblast-seeded membranes were investigated in the diffusion chamber. (*B*) Permeability coefficients (P_e) of phenol red for gelatin membranes after different pre-treatments: without cells; 7, 14 and 21 days with cells; and 21 days only with medium and without cells. Exposure to cells increased the permeability much more than incubation with buffer in the absence of cells.

3.2. Microstructure alterations of gelatin membranes

For a mechanistic understanding of how the permeability of biomaterials is modified by biological impacts, it is most instructive to perform a microstructural analysis. Consequently, gelatin membranes that had been exposed to cells were fixed, cryosectioned and stained to elucidate the membrane structure. Naive gelatin membranes displayed a homogeneous non-structured matrix with a fairly smooth surface (figure 3(*A*)). Under the influence of a confluent fibroblast monolayer as viewed in whole mount preparations (figure 3(*E*)) over a 1 week period, the gelatin surface became rough with irregular depressions, as deduced from cross sections of membranes. Most surprising was the occurrence of multiple cavities in innermost membrane regions (figure 3(*B*)). Obvious material loss, as judged from cryosections, was 2.3 times more pronounced in the gelatin proper than on the membrane surface (52.54 ± 13.64 kPi versus 22.64 ± 0.66 kPi). After 10 days of exposure to cells, involutions of variable depths evolved at the membrane surface, which, however, in no case penetrated the membrane diameter as a whole (figure 3(*C*)). Control specimens that were kept in the culture medium for 10 days without fibroblasts displayed hardly any surface alterations and internal holes.
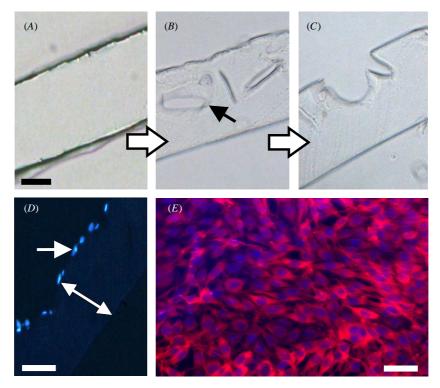
Figure 3. Structural analysis of gelatin membranes after cell exposure. (*A*)–(*C*) Phase contrast images of cross-sections of gelatin membranes in the absence of fibroblasts (*A*), after culturing with fibroblasts for 7 days (*B*) and for 10 days (*C*). Arrow in (*B*) marks a cavity formed in culture. (*D*) Blue DAPI staining of fibroblast nuclei of a gelatin membrane cross-section after 10 days culturing. Cells are restricted to the membrane surface (arrow) and do not penetrate the width of the membrane (two-headed arrow). (*E*) Top view of a fibroblast-seeded gelatin membrane. As judged from the actin filament staining with fluorescently labelled phalloidin, fibroblasts spread confluently on the membrane surface. Bar: (*A*) for (*A*)–(*C*) 40 μm, (*D*) 50 μm, (*E*) 20 μm.

In order to investigate whether cells had invaded the gelatin membrane and thus directly caused the formation of cavities, we stained cell nuclei which allowed us unequivocally to locate fibroblasts (figure 3(*D*)). After 10 days of culturing, cells were strictly confined to the surface of gelatin membranes without any direct contact to internal cavities. Consequently, it is very unlikely that cell surface-associated proteases had paved the way for invading fibroblasts and concomitant elaboration of cavities. Alternatively, cells could have released gelatin-degrading enzymes that did not affect more superficial membrane layers with a presumably higher rate of crosslinking (see section 4).

3.3. Proteolytic activity of cells

To address this question of whether the fibroblasts used in our experiments synthesized gelatin-degrading enzymes, a specific biochemical analytical method was employed. Fibroblasts were cultured as a confluent monolayer on gelatin membranes and the supernatant collected for subsequent electrophoresis in gelatin-acrylamide gels. After electrophoretic separation, proteins were renatured within the gel by selected incubation overnight. During this period, the gelatin gel became degraded selectively at those sites where gelatin-degrading proteins had been focused electrophoretically. As the image of a Coomassie-stained gel illustrates, fibroblast supernatants contained various proteinases with molecular weights of 55 kDa, 62 kDa and 65 kDa, in addition to

some unidentified high molecular weight proteases or isoforms (figure 4). Since the addition of a specific matrix metalloproteinase inhibitor prevented the formation of most gel bands, we conclude that the bulk protease activity was related to MMPs. The molecular weights indicated corresponded to MMP-8 (collagenase), and gelatinases MMP-2 and MMP-9 in their active form, respectively. The data are in agreement with the assumption that fibroblasts secreted proteases of the MMP type, which were likely to cause vacuole formation inside gelatin membranes. This in turn could account for the time-dependent permeability increase.

4. Discussion

4.1. The diffusion device

Our methodology provides a means of analysing gelatin membranes with respect to their permeability for molecular components and transmigratory cells. Employing a two-chamber system, we find that the investigated membrane displays (1) semipermeability for a molecular marker, (2) no permeability for cells and (3) an increase in marker permeability with time which is about one order of magnitude larger in the presence of cells. A prerequisite for such an analysis is the combination of cell culture and diffusion tests.

Since the test period comprised an 8 h exposure to the molecular diffusion marker, the chamber and its
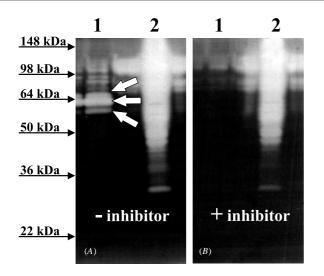
Figure 4. Protease release of fibroblasts. Fibroblasts were cultured on gelatin membranes and the supernatant collected for electrophoresis in gelatin-containing polyacrylamide gels (lanes 1). Purified non-MMP proteases (collagenase B) was used as positive control in zymography (lanes 2). The gel in the absence (*A*) and presence (*B*) of the matrix metalloproteinase (MMP) inhibitor. In the presence of proteases, gelatin is degraded and becomes visible after staining. Fibroblasts synthesized proteases of different molecular weights, some of which correspond to the active forms of matrix metalloproteinases MMP-8 (55 kDa), MMP-2 (62 kDa) and MMP-9 (65 kDa) (arrows in (*A*)). In the presence of the MMP inhibitor these bands are missing, but not those of the non-MMP proteases (lane 2 in (*B*)).

application needed to be fully biocompatible. We had initially employed the chamber device to investigate blood–retina barrier characteristics. For this purpose, tissue sheets of the retinal pigment epithelium were used as an interface between the two half-chambers, and the passage of pharmaceuticals was quantified by mass spectrometry [23, 24]. Incubation lasted for no longer than 1 h. In the current approach, the exposure time of gelatin membranes seeded with cells was extended to 8 h within the chamber without any obvious signs of cell stress. The possibility of immobilizing membranes by two o-rings that could be integrated into the polycarbonate chamber blocks was very helpful. Thus, it became feasible to handle ultrathin gelatin membranes on which fibroblasts had been cultured for up to 3 weeks in regular culture dishes, before cell-coated membranes in o-rings were transferred to the diffusion chamber.

This system has been recently employed to culture human bone-marrow-derived stromal cells on membranes of biomimetically mineralized collagen type I. It was possible to perfuse both half-chambers separately and constantly with the culture medium via the four outlets [26, 27]. Alternatively, the system is suitable for biomaterial testing of potential lung implants, because air–liquid interfaces can also be realized: A549 epithelial lung cells have been cultured on non-resorbable membranes and used to investigate airborne ultrafine carbonaceous particles [28]. Finally, the two-chamber system could be employed to test the biomaterial performance encountering variable hydrostatic pressures as evident during physiological and pathological blood flow.

Using endothelial or distinct epithelial cells reflecting the luminal lining of the vasculature and kidney, *in vivo*-like permeability tests of biomaterials become feasible [29].

However, some limitations need to be considered. During long-term perfusion culturing, a major obstacle is micro-injuries in the cell lining caused by gas bubbles, which randomly accumulate at the luminal or abluminal interface. Additionally, edge damages might occur where cells approach o-ring surfaces. A number of troubleshooting considerations have been proposed such as the introduction of a gas expander module to separate gas bubbles from the liquid phase without reduction of the oxygen pressure and special handling of o-rings harbouring membranes [30].

For the acquisition of permeability data, we found it to be advantageous to rely on the passage of phenol red, which was quantified by photometric means at 558 nm. However, other markers could be used, e.g. radioactive compounds with incorporated ^{35}S in conjunction with subsequent scintillation counting, specific proteins with Western blot analysis or enzyme-linked immunosorbent assays, and tracer components quantified by HPLC/mass spectrometry. However, in all cases the detection limits (especially in the acceptor chamber) need to be carefully considered. Only minute amounts of the marker are applicable, because the total volume of each half-chamber of the device is only about 0.5 ml.

4.2. Histological analysis

Cryosectioning and cell staining the specimens showed that gelatin membranes (1) retained their barrier function for invading cells during the investigated time period *in vitro* and (2) developed cavities in the membrane proper without any direct connection to membrane surfaces.

Our observations emphasize the value of histological analyses, because only evaluation at the micrometre level allows such an unexpected phenomenon to be revealed. The membrane became degraded only at a distance from cells which obviously caused cavity formation, since in the absence of cells no cavities became evident. The causal link is likely to originate from the two-step production process of membranes. In the first step, gelatin membranes were synthesized by mixing gelatin and methanal in a liquid phase followed by dehydration. In the second step, crosslinking of hydrolyzed collagen molecules was further enhanced by the exposure of gelatin membranes to methanal vapour. Whereas the first crosslinking step was ubiquitous, the second crosslinking step was initiated at the membrane surface and proceeded into deeper membrane layers. Obviously, a gradient of crosslinking resulted from this process with more stable surface layers and labile internal layers. Thus, the membrane inside became affected first by cellular enzymes and not the membrane surface. An alternative explantation could be that preexisting micropores allowed the infusion of enzyme and subsequently primary degradation from the interior of gelatin membranes. In summary, the histological analysis not only suggests mechanistic aspects of material processing but in turn provides information about how to change parameters for an alternative biomaterial profile.

4.3. Enzymatic degradation of membranes

Zymograms of media conditioned by fibroblasts on gelatin membranes pointed to the presence of distinct MMPs. The released MMPs are probably the cause of the slow degradation of the gelatin matrix. Since the crosslinks in gelatin membranes are more stable at their surface, primary degradation will be expected to be observed in the inner membrane layers, assuming that macromolecular proteins penetrate the gelatin matrix.

Since the expression of MMPs has been shown to depend partly on the exposure of cells to the corresponding extracellular matrix components that represent targets of these MMPs [31, 32], it is essential to seed the corresponding cells on the biomaterial to be tested. Testing relevant cells on irrelevant substrata might provide artefacts. After having identified the biomaterial degrading proteinase class, peptide linkers could be used as biomaterial crosslinkers that are either specifically cleavable or resistant to the defined enzymatic degradation [33–35]. Alternatively, the degradation kinetics of resorbable biomaterials could be modified by pharmacological intervention. Thus, specific protease inducers or antagonists could be incorporated into biomaterials and reduce or prolong, respectively, implant stability [36–38]. In this way, implant resorption could differentially be guided in different tissues or according to different pathophysiological conditions such as inflammation.

5. Conclusions

The permeability of biomaterials is crucial for a number of implant types and applications. It can be easily tested in conjunction with various monitoring procedures in a two-chamber device, which, in combination with cell culturing, allows distinct aspects of the *in vivo* situation to be mimicked. Thus, implant development is likely to be accelerated and simultaneously, animal experimentation can be reduced. Additionally, histological evaluation allows a special analysis at a micro level, which in turn provides a means of qualifying details of biomaterial processing. Finally, zymography provides insight into cell responses to selected biomaterials on the molecular level. Data obtained this way could be used to modify implant concepts from a mechanistic point of view and thus follow a somewhat similar rationale as in drug development strategies [39].

Acknowledgments

References

[1] Hillaireau H *et al* 2007 Encapsulation of mono- and oligo-nucleotides into aqueous-core nanocapsules in presence of various water-soluble polymers *Int. J. Pharm.* **331** 148–52

[2] Schmidt P G *et al* 2007 PEGylated bioactive molecules in biodegradable polymer microparticles *Expert Opin. Biol. Ther.* **7** 1427–36

[3] Lindvall O and Wahlberg L U 2008 Encapsulated cell biodelivery of GDNF: a novel clinical strategy for neuroprotection and neuroregeneration in Parkinson's disease? *Exp. Neurol.* **209** 82–8

[4] Murua A *et al* 2007 In vitro characterization and in vivo functionality of erythropoietin-secreting cells immobilized in alginate-poly-l-lysine-alginate microcapsules *Biomacromolecules* **8** 3302–7

[5] Rinsch C *et al* 2002 Delivery of erythropoitin by encapsulated myoblasts in a genetic model of severe anemia *Kidney Int.* **62** 1395–401

[6] Rinsch C *et al* 2001 Delivery of FGF-2 but not VEGF by encapsulated genetically engineered myoblasts improves survival and vascularization in a model of acute skin flap ischemia *Gene Therapy* **8** 523–33

[7] Peduto G *et al* 2000 Long-term host unresponsiveness to encapsulated xenogeneic myoblasts after transient immunosuppression *Transplantation* **70** 78–85

[8] Rinsch C *et al* 2001 Inducing host acceptance to encapsulated xenogeneic myoblasts *Transplantation* **71** 345–51

[9] Joseph J M *et al* 1994 Transplantation of encapsulated bovine chromaffin cells in the sheep subarachnoid space: a preclinical study for the treatment of cancer pain *Cell Transplant.* **3** 355–64

[10] Sagen J *et al* 1993 Transplants of immunologically isolated xenogeneic chromaffin cells provide a long-term source of pain-reducing neuroactive substances *J. Neurosci.* **13** 2415–23

[11] Zurn A D *et al* 2000 Evaluation of an intrathecal immune response in amyotrophic lateral sclerosis patients implanted with encapsulated genetically engineered xenogeneic cells *Cell Transplant.* **9** 471–84

[12] Norton L W *et al* 2005 In vitro characterization of vascular endothelial growth factor and dexamethasone releasing hydrogels for implantable probe coatings *Biomaterials* **26** 3285–97

[13] Ye S H, Watanabe J and Ishihara K 2004 Cellulose acetate hollow fiber membranes blended with phospholipid polymer and their performance for hemopurification *J. Biomater. Sci. Polym. Ed.* **15** 981–1001

[14] Liu Y, Shu X Z and Prestwich G D 2005 Biocompatibility and stability of disulfide-crosslinked hyaluronan films *Biomaterials* **26** 4737–46

[15] Duan X and Sheardown H 2006 Dendrimer crosslinked collagen as a corneal tissue engineering scaffold: mechanical properties and corneal epithelial cell interactions *Biomaterials* **27** 4608–17

[16] Giraudier S *et al* 2004 Influence of weak and covalent bonds on formation and hydrolysis of gelatin networks *Biomacromolecules* **5** 1662–6

[17] Schlosshauer B and Lietz M 2004 Nerve guides *Encyclopedia of Biomaterials and Biomedical Engineering* ed G E Wnek and G L Bowlin (New York: Dekker) pp 1043–55

[18] Schlosshauer B *et al* 2006 Synthetic nerve guide implants in humans: a comprehensive survey *Neurosurgery* **59** 740–7; discussion 747–8

[19] Lietz M *et al* 2006 Physical and biological performance of a novel block copolymer nerve guide *J. Biotech. Bioeng.* **5** 99–109

[20] Rutkowski G E and Heath C A 2002 Development of a bioartificial nerve graft I. Design based on a reaction-diffusion model *Biotechnol. Prog.* **18** 362–72

[21] Atkins S *et al* 2006 Scarring impedes regeneration at sites of peripheral nerve repair *Neuroreport* **17** 1245–9

[22] Ozgenel G Y 2003 Effects of hyaluronic acid on peripheral nerve scarring and regeneration in rats *Microsurgery* **23** 575–81

[23] Steuer H *et al* 2005 Functional characterization and comparison of the outer blood-retina barrier and the blood-brain barrier *Invest. Ophthalmol. Vis. Sci.* **46** 1047–53

[24] Steuer H *et al* 2004 In vitro model of the outer blood-retina barrier *Brain Res. Brain Res. Protoc.* **13** 26–36

[25] Stier H and Schlosshauer B 1995 Axonal guidance in the chicken retina *Development* **121** 1443–54

[26] Bernhardt A, Lode A, Boxberger S, Pompe W and Gelinsky M 2007 Mineralised collagen—an artificial, extracellular bone matrix—improves osteogenic differentiation of bone marrow stromal cells *J. Mater. Sci. Mater. Med.* **19** 269–75

[27] Minuth W W, Schumacher K and Strehl R 2005 Renal epithelia in long term gradient culture for biomaterial testing and tissue engineering *Biomed. Mater. Eng.* **15** 51–63

[28] Bitterle E *et al* 2006 Dose-controlled exposure of A549 epithelial cells at the air-liquid interface to airborne ultrafine carbonaceous particles *Chemosphere* **65** 1784–90

[29] Tan Q *et al* 2007 Accelerated angiogenesis by continuous medium flow with vascular endothelial growth factor inside tissue-engineered trachea *Eur. J. Cardiothorac. Surg.* **31** 806–11

[30] Minuth W W and Strehl R 2007 Technical and theoretical considerations about gradient perfusion culture for epithelia used in tissue engineering, biomaterial testing and pharmaceutical research *Biomed. Mater.* **2** R1–11

[31] Kim I Y *et al* 2007 Type I collagen-induced pro-MMP-2 activation is differentially regulated by H-Ras and N-Ras in human breast epithelial cells *J. Biochem. Mol. Biol.* **40** 825–31

[32] Tchetina E V *et al* 2007 Chondrocyte hypertrophy can be induced by a cryptic sequence of type II collagen and is accompanied by the induction of MMP-13 and collagenase activity: implications for development and arthritis *Matrix Biol.* **26** 247–58

[33] Gabriel D *et al* 2007 Tailoring protease-sensitive photodynamic agents to specific disease-associated enzymes *Bioconjug. Chem.* **18** 1070–7

[34] Vessillier S, Adams G and Chernajovsky Y 2004 Latent cytokines: development of novel cleavage sites and kinetic analysis of their differential sensitivity to MMP-1 and MMP-3 *Protein Eng. Des. Sel.* **17** 829–35

[35] Lutolf M P and Hubbell J A 2005 Synthetic biomaterials as instructive extracellular microenvironments for morphogenesis in tissue engineering *Nat. Biotechnol.* **23** 47–55

[36] Buss A *et al* 2007 Matrix metalloproteinases and their inhibitors in human traumatic spinal cord injury *BMC Neurol.* **7** 17

[37] Li Y *et al* 2006 TNF-alpha up-regulates matrix metalloproteinase-9 expression and activity in alveolar macrophages from patients with chronic obstructive pulmonary disease *J. Huazhong Univ. Sci. Technol. Med. Sci.* **26** 647–50

[38] Krzeski P *et al* 2007 Development of musculoskeletal toxicity without clear benefit after administration of PG 116800, a matrix metalloproteinase inhibitor, to patients with knee osteoarthritis: a randomized, 12 month, double-blind, placebo-controlled study *Arthritis Res. Ther.* **9** R109

[39] Lalonde R L *et al* 2007 Model-based drug development *Clin. Pharmacol. Ther.* **82** 21–32